TEM Sample Preparation and FIB-Induced Damage

Joachim Mayer, Lucille A. Giannuzzi, Takeo Kamino, and Joseph Michael

Abstract

One of the most important applications of a focused ion beam (FIB) workstation is preparing samples for transmission electron microscope (TEM) investigation. Samples must be uniformly thin to enable the analyzing beam of electrons to penetrate. The FIB enables not only the preparation of large, uniformly thick, site-specific samples, but also the fabrication of lamellae used for TEM samples from composite samples consisting of inorganic and organic materials with very different properties. This article gives an overview of the variety of techniques that have been developed to prepare the final TEM specimen. The strengths of these methods as well as the problems, such as FIB-induced damage and Ga contamination, are illustrated with examples. Most recently, FIB-thinned lamellae were used to improve the spatial resolution of electron backscatter diffraction and energy-dispersive x-ray mapping. Examples are presented to illustrate the capabilities, difficulties, and future potential of FIB.

Introduction

Whereas the initial development of focused ion beam (FIB) instruments was driven by their unique capabilities for computer chip repair and circuit modification in semiconductor technology, present FIB applications support a much broader range of scientific and technological disciplines (for an overview, see Reference 1). However, despite their huge potential in many different areas, ranging from top-down structuring in nanotechnology to tomographic characterization in complex microstructures, many FIBs are largely used to prepare transmission electron microscope (TEM) cross-section sample lamellae. This article explores why FIB preparation of TEM samples in many laboratories has largely displaced ion millers despite the enormous financial investment and the artifacts created by FIB-induced damage.

The main advantages of using an FIB for TEM specimen preparation are

- No other technique can select the target area as precisely as FIB; that is, with care, lamellae can be prepared with a spatial accuracy of within ~20 nm.
- FIB preparation is fast and reliable; in as little as 20 minutes and within a maximum of 2–4 hours, specimens of an almost unlimited range of materials can be prepared.
- FIB preparation techniques are virtually independent of the nature of the material. Owing to the special geometry and the specific properties of the protective cover on the surface, the milling procedures require only minor adjustments, if at all, that are dependent on the bulk properties of the material.

Special techniques for semiconductors have been developed that offer optimized solutions in terms of speed, reliability, damage removal, or total electron transparent area. On the other hand, it is widely recognized that FIB specimen preparation can be applied to almost any material type—hard, soft, or combinations thereof. The number of materials for which successful TEM sample preparation with FIBs has been documented certainly reaches several hundred and spans from hard matter such as metals, ceramics, and composites to soft matter including polymers, biological materials, and even frozen liquids.

The main disadvantage of FIBs, however, is caused by the nature of the milling process: the ion collisions initiating sputter removal can also lead to ion implantation and cause severe damage to the remaining bulk of the material. As the FIB lamellae method spreads to more advanced TEM techniques, various procedures have been developed to reduce or repair this damage.

In this article, the major specimen preparation techniques are reviewed; the consequences of FIB-induced damage are discussed, along with strategies to reduce the damage; and an overview on applications in materials science and in related instrumental fields is presented.

Specimen Preparation Techniques

Since the first-generation FIBs were mainly used as semiconductor tools, early attempts to prepare TEM specimens in an FIB also focused on semiconductor materials. The initial methods were based on mechanically polishing the sample down to an approximately 50-µm lamella and then using the FIB to cut two trenches, one from each side, leaving behind a thin electron-transparent lamella supported by bulk material on two opposite sides (Figure 1).[2] Referring to the geometry seen in Figure 1, this method is frequently called the H-bar technique. This method was subsequently refined by employing a tripod polisher for the initial thinning of the thin slab,[3] which is particularly valuable in the case of complex semiconductor devices.

In parallel, techniques were developed that make it possible to directly remove an electron-transparent lamella from a bulk specimen without mechanical polishing (see Figure 2). These so-called lift-out techniques were first proposed by Overwijk et al.[4] and further developed to a routinely and reliably applicable technique for a broad materials range by Giannuzzi et al.[5] Whereas the first attempts were based on an *ex situ* lift-out of the lamella using a micromanipulator under an optical microscope, techniques based on an *in situ* lift-out of the lamella are gaining increasing importance.[6] Specimens extracted by *in situ* lift-out can be shaped in a number of different and

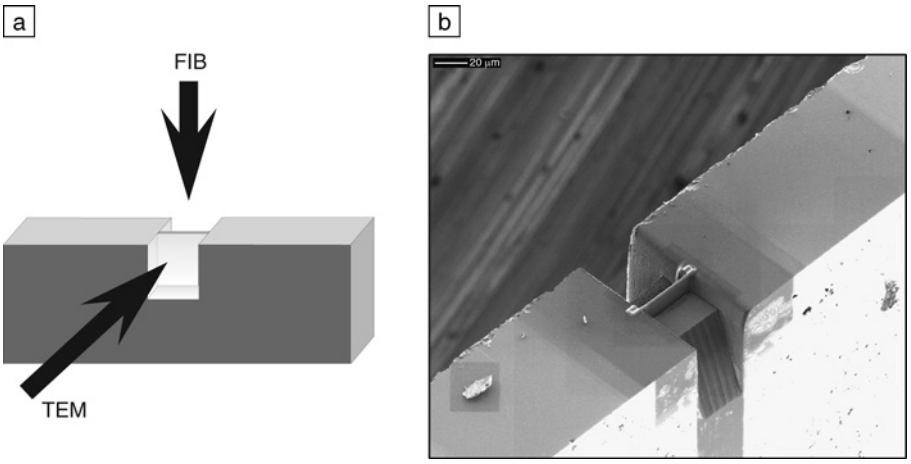

Figure 1. (a) Schematic illustration of the H-bar focused ion beam (FIB) technique. Material on opposite sides of a region of interest is FIB-milled until it is electron-transparent. (b) Scanning electron microscopy (SEM) image showing the top-down view of an H-bar FIB specimen in progress. The metal sample was mechanically thinned to ~40 µm and glued to a transmission electron microscope (TEM) half-grid. (Figure courtesy of Richard Young, FEI Co.)

very useful geometries and can be treated with low-energy gallium or argon ions for further thinning and removal of FIB-induced damage.[7]

In the next three sections, we introduce the techniques that require some pre-preparation, such as sectioning and polishing, and then focus on the more universal techniques based on a lift-out of a thin lamella from an otherwise unmodified piece of material.

Methods Requiring Pre-Thinning

In this frequently applied case, the initial specimen must first be trimmed mechanically before the sample is placed in the FIB for milling. In the most commonly used version of this technique,[2,8,9] a thin slab of the material is cut from the area of interest in the sample and mechanically polished as thin as possible. The sample material is then mounted on a half-grid and inserted vertically into the FIB chamber. Before cutting, a W or Pt line is usually deposited on the area of interest to protect the top portion of the specimen and to mark the position of the target area. After cutting two deep trenches, the final lamella, if seen from the top, looks like the crossbar in the letter "H" (Figure 1). The technique is thus commonly referred to as the H-bar technique and is still frequently used in the semiconductor field, particularly when combined with a fast and efficient microcleavage tool.

This conventional technique was further improved by its combination with tripod polishing.[3,10,11] Reducing the thickness of the initial piece of material to only 2–3 µm or less in the volume of interest offers several advantages, such as reduced FIB milling time and a reduced fluorescence yield contribution from the neighboring material in analytical TEM investigations with energy-dispersive x-ray analysis (EDX). A modified version of this technique can also be used to prepare plan-view specimens.[11]

Ex Situ *Lift-Out*

In the *ex situ* lift-out (EXLO) technique, a freestanding site-specific region is FIB-milled to electron transparency, and then the thin lamella is removed from its trench with a micromanipulator under an optical microscope.[5,8] The specimen attaches to the micromanipulator tip via electrostatic forces and can be removed easily from its trench. EXLO specimens can be transferred to carbon-coated TEM grids, formvar-coated grids, holey carbon grids, or directly to the surface of small mesh grids. Automated routines were developed to increase throughput and enable automated FIB specimen preparation.[12–15] This technique was first exploited for cross-sectional TEM analysis. Depending on the geometry of the starting sample, cross-sectional specimens may be FIB-milled either perpendicular to or parallel to the substrate. Plan-view specimens may also be prepared by directly FIB-milling specific layers parallel to the beam. Alternatively, EXLO plan-view specimens may be prepared using a two-step FIB-milling and lift-out step.[16] An advantage to the EXLO method is that it is very fast and often satisfactory for conventional TEM analysis. Disadvantages to the EXLO technique are that it is very difficult (if not impossible) to further thin the EXLO specimen once it is mounted to a coated grid; the grid coating can hinder certain TEM analyses such as electron holography and energy-filtered microscopy; and the FIB operator must be careful to avoid redeposition artifacts on the EXLO specimens, because final FIB milling is performed while the specimen is still confined within a trench.

In Situ *Lift-Out/Microsampling*

The microsampling method[17–19] and the *in situ* lift-out (INLO) techniques[1,20] are very similar and consist of extracting and transferring a small wedge-shaped or parallel-sided piece of sample via an internal nanomanipulator to a TEM half-grid while it is still inside the FIB chamber. Final FIB milling is performed when the sample is on the TEM grid. The *in situ* manipulation is enabled by the FIB deposition of a metal layer to first "glue" the manipulator probe to the sample and then to glue it to the grid. FIB milling to electron transparency then progresses in a similar fashion as for an H-bar specimen. As an example, a very large (i.e., 80 µm long) INLO wedge of material from a Cu-Ni diffusion couple and the subsequently FIB-thinned TEM specimen are shown in Figures 2a and 2b.[21] For such long lamellae, sufficient stability can only be achieved when the lamellae are mounted from the top to a TEM half-grid (Figure 2b). For shorter lamellae, it is advantageous to mount the piece from the side to a special support grid (Figure 2c).

A modified version of the microsampling or INLO method can be used to prepare a plan-view specimen from a specific site, as shown in Figure 3. First, the area to be observed in plan view is cut out, and a small wedge-shaped piece of sample is extracted from the site (Figure 3a). The extracted sample is then transferred (Figure 3b) and mounted (Figure 3c) onto the edge of a carrier grid. Subsequently, the carrier grid is rotated by 90° for thinning parallel to the sample surface (Figure 3e). The e^- beam direction is shown in Figure 3f.

FIB-Induced Damage and Removal Techniques

The ion impact on the specimen surface not only leads to material removal by the sputtering process, but also to the formation of a damaged layer that may extend several tens of nanometers into the material (see also the introductory article by guest editors C.A. Volkert and A.M. Minor in this issue). Whereas this may easily be understood for ions that impinge at normal incidence onto the sample surface,

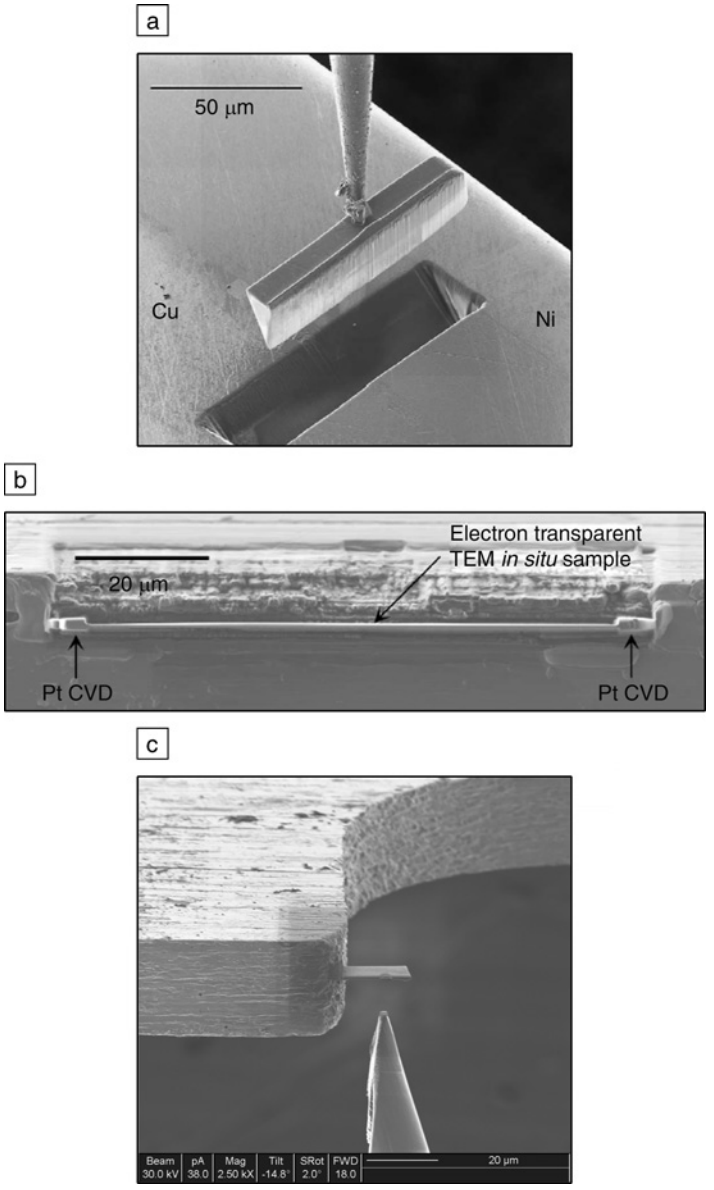

Figure 2. *In situ* lift-out of a sample piece by means of a nanomanipulator mounted inside the FIB chamber. (a) An 80-μm-long piece of material is mounted to the nanomanipulator needle by Pt deposition. (b) After transfer, the lamella is mounted from the top to a TEM half-grid and finally thinned to electron transparency. (c) Shorter lamellae are mounted from the side to the central posts in special half-grids.

momentum transfer and Ga implantation into the bulk may even occur for ions that are used for milling at glancing angles of <1°. The result may range from complete amorphization, as in the case of semiconductor materials, to the formation of defect agglomerates and even intermetallic phases, in the case of certain metals.

In semiconductor materials, the thickness of the amorphous layer formed on the FIB-prepared sample surfaces is nearly proportional to the range of Ga ion implantation,[22–24] which in turn is roughly proportional to the primary energy of the Ga ions. FIB columns that can be operated at accelerating voltages as low as 1–2 kV have recently become available. Thus, low-energy Ga milling is now available, and the effect of radiation damage and amorphization can be studied across a broad range of ion energies. Figure 4 shows the reduction of amorphous layer formation in a sidewall of Si as a function of Ga energy obtained from FIB milling at an 88° incident angle. For ion energies of 30 keV, 5 keV, and 2 keV, the observed sidewall damage is ~22 nm, 2.5 nm, and 0.5–1.5 nm, respectively.[7] The sidewall damage reduction in Si at 2 keV polishing can produce TEM specimens that reveal sub-angstrom information.[7]

The advantage to using the FIB is that the specimen can be imaged for exact placement of the final polishing window. In a DualBeam™ instrument, the low-energy FIB polishing can be directly monitored in SEM mode. Similar low-energy FIB techniques have been used to prepare specimens for atom probe analysis, where results show that no deleterious ion mixing occurs and no detectable Ga is present after final polishing with 2 keV Ga^+.[25]

Alternatively, low-energy ion milling with a broad Ar ion beam can be used to remove damage layers created by the FIB during lamellae formation and also to further reduce the specimen thickness.[12,26,27] Special ion polishers are in development that will enable milling to a controlled final specimen thickness. The ideal specimen thickness depends on the type of TEM technique and is usually 20–30 nm for electron energy loss spectroscopy analysis and should be less than 10 nm for a quantitative atomic-resolution TEM study, values which can now be reached in a final polishing step.

Whereas surface amorphization is the main concern in semiconductor materials, there have been several reports in the literature that FIB milling of fine-grained fcc metals can change the orientation and size of the surface grains and form Ga intermetallic compounds.[28–30] The extensive use of FIB milling for sample preparation and the use of ion channeling contrast to characterize and measure grain sizes require that these ion beam–induced modifications be properly understood.

The extreme microstructural modifications that can be caused by FIB are illustrated using an example for polycrystalline Cu. Sputter-deposited Cu films were exposed to various doses of 30 kV Ga^+ ions in the FIB and then cross-sectioned by the EXLO method for TEM, scanning transmission electron microscopy (STEM), and electron backscatter diffraction (EBSD) investigations. Figures 5a and 5c show examples of the Cu grain structure modification to a depth of 200 nm by an ion dose of 2.5×10^{17} Ga/cm^2, despite the fact that calculated ranges for 30 kV Ga ions are close to 50 nm (Figure 5b).[29] EBSD orientation mapping of the sample shows that the surface grains are reoriented so that the ⟨110⟩ direction, the strong channeling direction in fcc crystal structures, is oriented parallel to the incident ion beam, as shown in Figure 5c. Similar effects were observed in other fcc

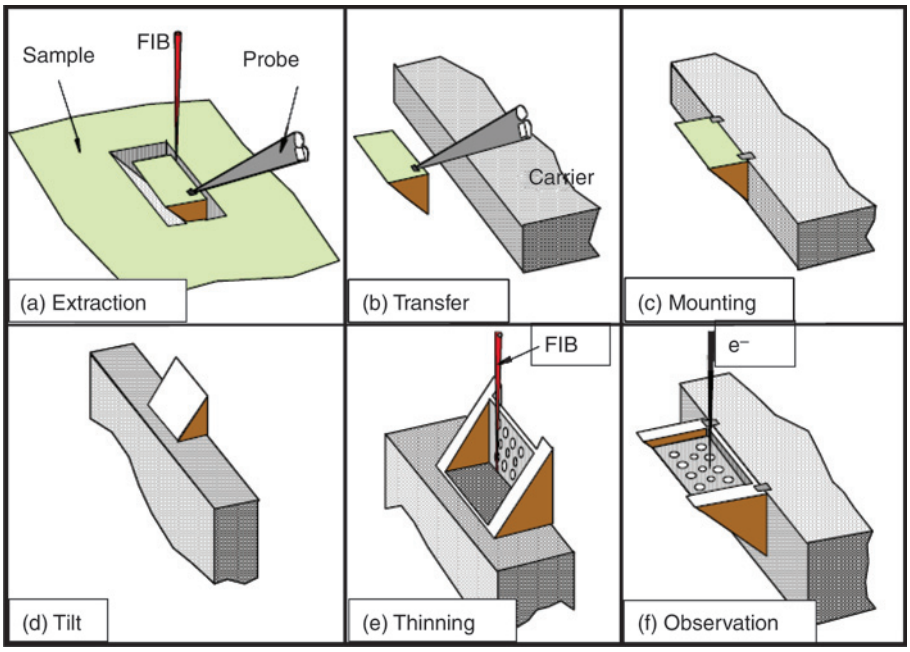

Figure 3. Method to prepare a plan-view specimen from a specific site based on the microsampling technique (see text for details).

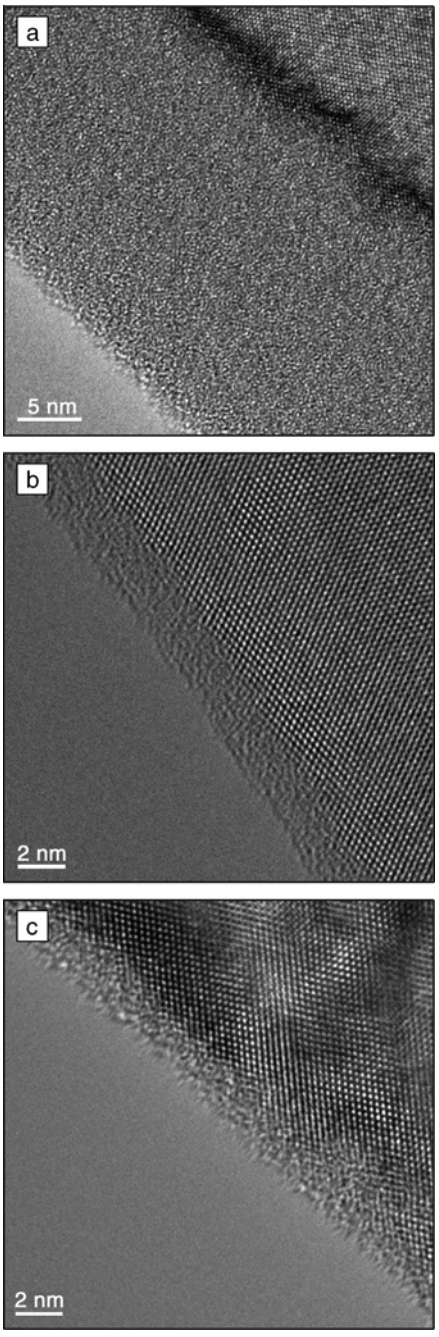

Figure 4. Reduction of the amorphous layer thickness in a sidewall of Si as a function of Ga energy. The cross sections of FIB lamellae show that FIB-milling at an 88° incident angle and 30 keV, 5 keV, and 2 keV ion energy results in amorphous layers of (a) ~22 nm, (b) 2.5 nm, and (c) 0.5–1.5 nm thickness, respectively.

metals (Au, Ni), and bcc metals were observed to reorient at the surface with a ⟨111⟩ crystallographic direction normal to the exposed surface.[5,31]

This work demonstrates that 30 kV Ga^+ ion exposure can cause extensive microstructural modification of metal samples, even to depths beyond the expected, non-channeling-orientation, ion range. Until these effects are understood and/or catalogued, caution should be used when FIB is employed to prepare samples for microstructural investigation, as even short exposures can result in unwanted changes to the sample.

One must also be careful that the implantation of Ga into the sample does not result in changes induced by the formation of new Ga-containing phases. The addition of Ga to many metals can result in low-melting temperature phases. Cu_3Ga has been observed at the bottom of FIB-milled trenches in Cu.[28] Thin TEM samples prepared from Al may show Ga enrichment at the grain boundaries. In extreme cases, because of its low melting point, Ga can form phases with other metals that have melting points at or below room temperature. For example, Ga addition during ion milling to In results in eutectic formation, with a melting temperature of 15.3°C. Thus, the potential exists to have a liquid phase present in Ga FIB-milled samples of In. The addition of 2.5 at.% Ga to Ge will also result in liquid-phase formation. Other metals, like Al, Zn, and Pb, have similar problems.[32] It is highly recommended the phase diagram be reviewed before FIB-milling new materials with Ga to avoid problem materials or prepare them in a different manner.

Applications to Different Classes of Materials

One of the main advantages of the FIB technique in many different applications is the accurate selection of the site and the cutting and thinning directions of the sample, enabling TEM investigation of precisely the desired location. Another important advantage is the fact that cross sections can successfully be prepared from almost any given combination of materials, inorganic or organic, hard or soft. As a first example, Figure 6 shows cross sections from a complex semiconductor device[17] and from a multilayer coating on the inner side of a light bulb.[33]

The semiconductor field is one of the main application areas for cross-sectional TEM, and as the characteristic dimensions of the latest devices have become smaller than 100 nm, FIB milling is the most practical and effective method of preparing site-specific samples. The accuracy requirements, particularly in nanoelectronics, for precisely locating an object in a TEM cross section increase dramatically. As an example, Figure 7 shows the results of cross-section investigations of a metal oxide semiconductor–based transistor with critical dimensions in the 10 nm range.[34,35] The vertical gate contact, structured using e-beam lithography, spans the source–drain line with a width of 200 nm.[34] The required accuracy for positioning an

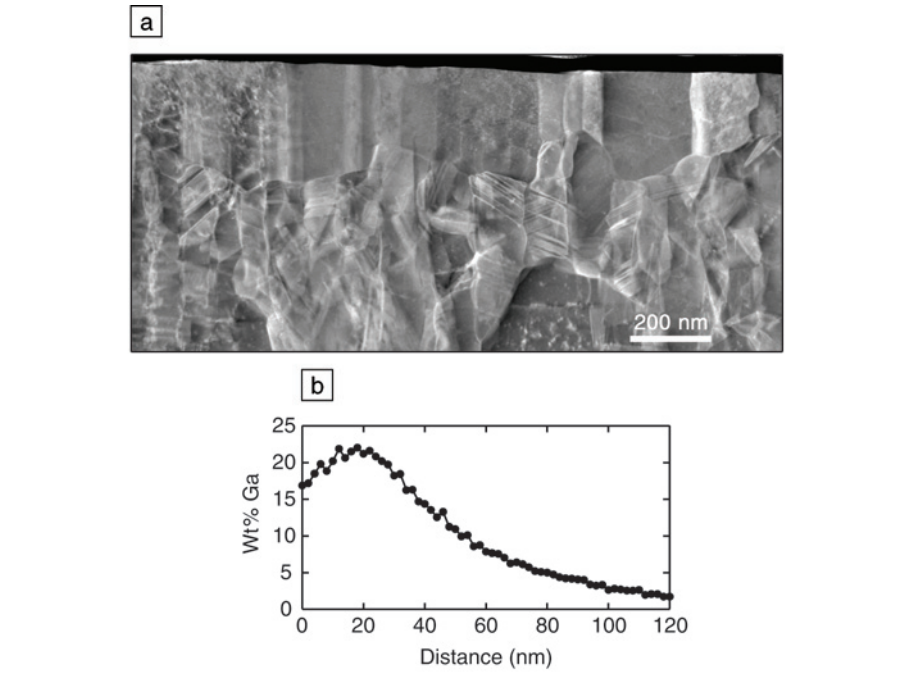

Figure 5. Sputtered Cu after exposure to a Ga^+ ion dose of 2.5×10^{17} ions/cm^2 at 30 kV. (a) Scanning transmission electron microscopy (STEM) image of an FIB-prepared cross section of the surface region. (b) Ga concentration as a function of distance from surface. (c) Electron backscatter diffraction (EBSD) orientation map with respect to exposed surface normal.

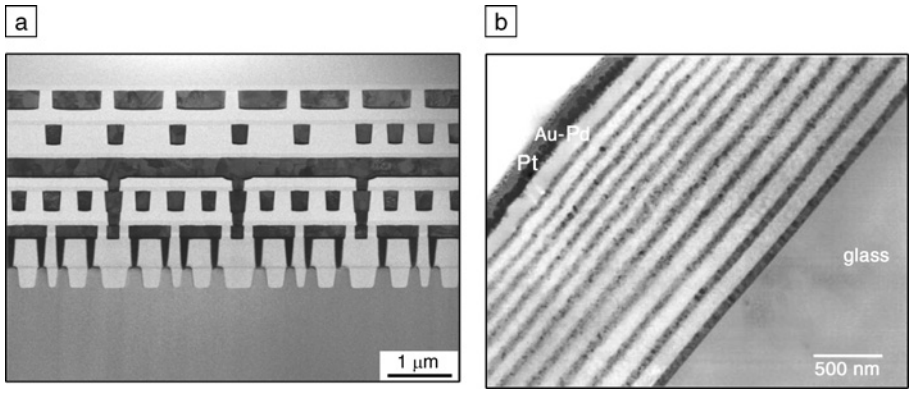

Figure 6. (a) FIB-prepared TEM sample of a Si device sliced and thinned exactly at the desired position. (b) Multilayer metal/oxide coating on the inner surface of a light bulb.

FIB lamella that intersects the gate contact along the source–drain line is thus about 50 nm. Such accuracy can easily be reached on a modern FIB, as is demonstrated from the TEM image and the inserted elemental distribution image in Figure 7, which show the final transistor after encapsulating the gate in an oxide layer and deposition of the upper gate contact. The active length of the gate contact was determined to be 12.5 nm from the elemental distribution images.[35]

Powder particles and thin fibers frequently pose unsolvable problems to conventional thinning techniques. However, they may also be too small to be held or fixed on a specimen stub and do not remain stable during FIB milling. Several methods were developed for this purpose and are practically applied.[18,36,37] One of the most practical methods is the resin embedding method. To minimize the damage created during FIB milling, the embedded sample can first be coated with a metal deposition layer. Figure 8 shows a TEM image of an FIB-prepared cross section through a toner particle. The toner was placed on the sharp edge of a metal disk, and a protective layer was deposited on the sample before FIB milling. The metal deposition layer minimizes the sample heating caused by FIB irradiation, and the obtained toner shape and inorganic particle distribution in the toner was better retained than in a sample prepared by cryo-ultramicrotomy.

Samples prepared with the FIB typically contain several tens of square micrometers of thinned area. In comparison, the electron transparent area of a thin sample prepared by conventional ultramicrotomy techniques can be about one hundred times larger. Hence, for normal resin-embedded biological tissues, it does not make sense to use FIB-milling techniques. However, for the site-specific characterization of biological tissues, FIB sample preparation combined with STEM or TEM observation techniques can be very advantageous.

Before the FIB technique was put to practical use, TEM sample preparation of interfaces between hard and soft materials (such as semiconductor/polymer or metal/rubber) was one of the most difficult tasks and frequently could not be done successfully. One of the advantages of the FIB milling technique as compared to standard TEM sample preparation methods is the possibility of obtaining uniformly thick TEM samples from interfaces composed of very dissimilar materials. The feasibility of using a FIB for the purpose of thinning vitreously frozen biological specimens for TEM was explored

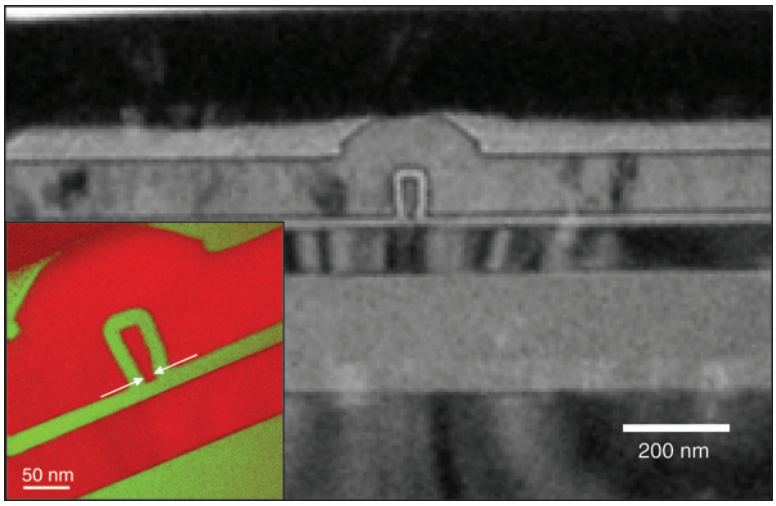

Figure 7. FIB/TEM investigations of a nanoscale metal oxide semiconductor field-effect transistor with a vertical gate design. TEM overview image of the final transistor in cross section and (inset) elemental distribution image obtained by energy-filtering TEM, showing the Si distribution in red (source–drain line, vertical gate, and upper gate) and the oxide layers in green. The active length of the gate is 12.5 nm (indicated by arrows in the inset).

in a study by Marko et al.[38] A concern was whether heat transfer beyond the direct ion interaction volume might devitrify the ice. In the studies, changes indicative of heat-induced devitrification were not observed by TEM, in either images or diffraction patterns. Hence, cryo-FIB thinning of bulk frozen-hydrated material may be used in the future with much greater efficiency than cryo-ultramicrotomy to prepare specimens for TEM cryo-tomography, without the specimen distortions and handling difficulties of the latter.

Related Fields of Application

The techniques for preparing TEM lamellae described in the section "Specimen Preparation Techniques" can be very useful for preparing specimens for other structural and analytical characterization techniques. As examples, we discuss applications in SEM, field ion microscopy, and three-dimensional atom probe (TAP) specimen preparation.

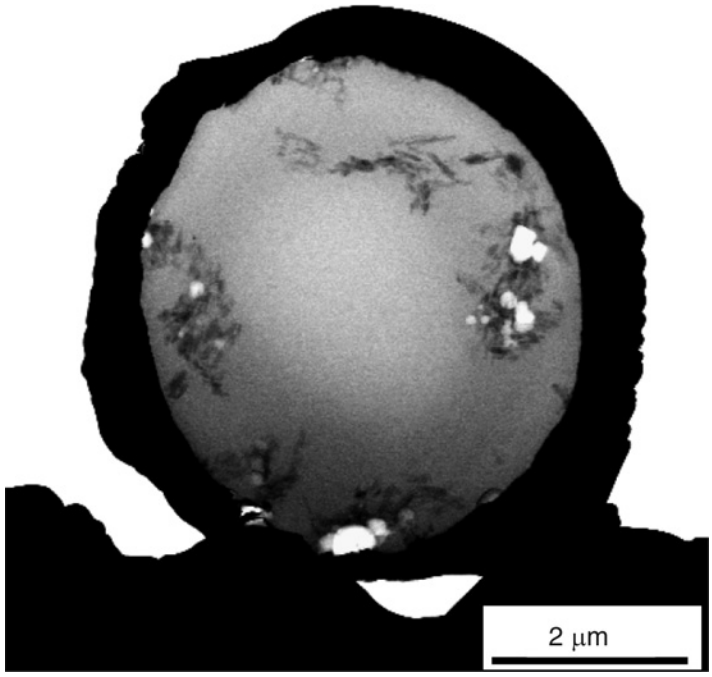

Figure 8. FIB-prepared toner sample placed on a metal disk and coated in preparation for FIB milling.

The main advantage of SEM as compared with TEM is the capability to analyze bulk specimens and large areas. However, there are SEM modes that can considerably benefit from using thin samples as a means to avoid the large interaction volume. By using FIB lamellae, the resolution in an EDX analysis can be dropped considerably below 100 nm, even at high accelerating voltages. Specimens prepared using INLO techniques are ideal for this purpose, and the analysis is particularly fast in a dual-beam instrument equipped with a an energy-dispersive spectroscopy detector. In the experiment, transmitted electrons must be captured in a material with a low x-ray production efficiency (e.g., a carbon substrate).

Transmitted electrons can also provide useful information about the specimen, not only in terms of the thickness of an FIB-prepared TEM lamella, but also with respect to the microstructure and phase composition. High-resolution FEG-SEM (field-emission gun SEM) or dual-beam instruments can now reach subnanometer resolution and with a STEM detector can provide information on the specimen at 30 kV using similar contrast mechanisms as in a higher-voltage 200–300 kV TEM, but in a much shorter time.

Another important field of application that has recently been demonstrated is the improvement in EBSD spatial resolution. EBSD of FIB-milled cross-section samples is possible, and the use of thin samples improves the spatial resolution of the technique.[39] Field-emission SEM and thin samples have enabled EBSD to achieve spatial resolutions that approach 10 nm. One interesting application of this high spatial resolution is in the study of austenite/ferrite microstructures that exist in certain types of iron meteorites. An important field of study in meteoritics is understanding the thermal history of a meteorite as inferred from the microstructure. In this case, both TEM and EBSD have played important roles.

There are regions of meteorites, called cloudy zones (based on their etched appearance in optical microscopy), where there is an intimate mixing of austenite and ferrite. EBSD orientation mapping of samples prepared by careful metallographic techniques was unsuccessful because of the small length scales of the microstructure. EXLO of thin TEM

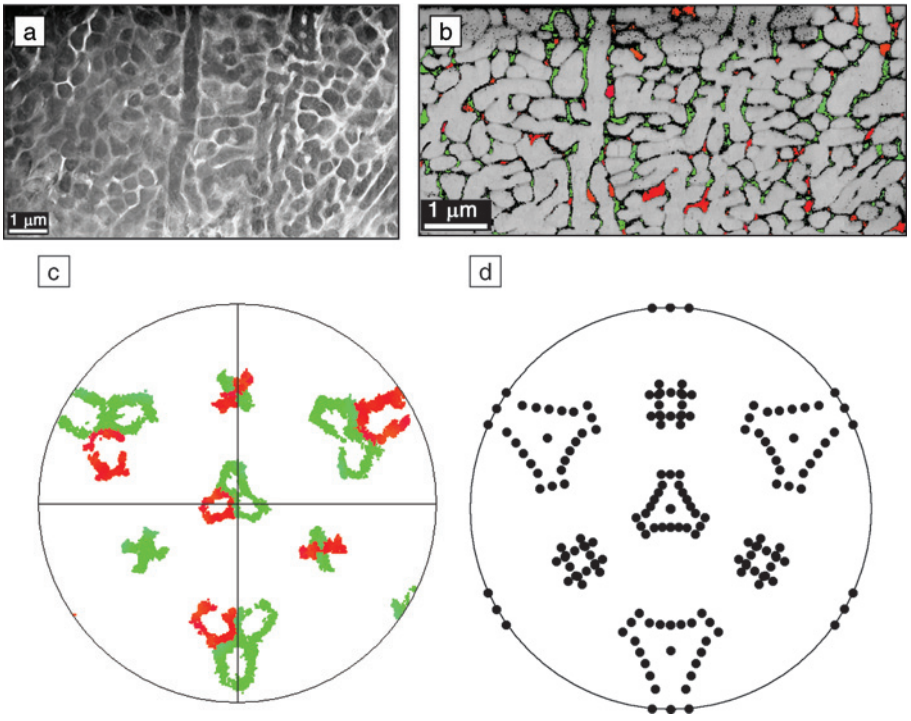

Figure 9. STEM and EBSD results of an FIB-prepared thin sample of the cloudy zone in a meteorite. (a) Annular dark-field STEM image; (b) EBSD map showing the ferrite in color; (c) [110] ferrite pole figure obtained from (b); and (d) [110] pole figure for ferrite, showing the distribution of poles expected from well-known austenite/ferrite orientation relationships.

lamellae was used to prepare samples of the cloudy zone for TEM and EBSD mapping. Figure 9a is an annular dark-field STEM image of the cloudy zone from an EXLO FIB sample that shows the distribution of the austenite and ferrite phases. Figure 9b is an EBSD orientation map obtained from the thin sample shown in Figure 9a. The area in gray tones is austenite of a single orientation, and the color-coded regions are ferrite. Note that the EBSD map was obtained with a step size of 10 nm. The EXLO FIB sample provided significantly better EBSD orientation mapping of the two-phase region than the metallographic sample. Figures 9c and 9d compare the experimental [110] ferrite pole figure obtained from the data shown in Figure 9b to the expected pole distribution based on the accepted descriptions of austenite/ferrite orientation relationships, where close-packed directions and close-packed planes of the austenite or ferrite are parallel. In this case, the use of FIB, STEM, and EBSD of the same sample regions allowed the fine-scale details of the microstructure to be studied and enabled a better understanding of the thermal history of the meteorite.

Field ion microscopy and TAP are widely recognized as powerful tools for the study of local atomic structure and local chemistry with single-atom sensitivity. However, the application of these techniques frequently suffers from the stringent requirements of the specimen geometry. An ideal specimen should form a sharp conical tip with an end radius of <50 nm and a taper angle of <5°.[40] Forming sharp needles with electropolishing techniques is the most frequently applied method to obtain suitable specimens.

Although these techniques work very well for many metals and alloys, they cannot be applied for the preparation of thin films and layered structures or site-specific specimens of grain boundaries or interfaces. In pioneering work, Larson et al.[41–43] demonstrated the potential of FIB for preparing TAP specimens from multilayered Co/Cu and related materials used for magnetic data storage. In recent years, many alternative techniques for tip preparation have been developed, an overview of which is given by Miller et al.[40] In particular, Miller et al. developed techniques based on INLO that make it possible to prepare site-specific specimens from a range of different materials. Perez-Willard[44] recently demonstrated that specimens containing a single crystallographically well-defined grain boundary can be prepared using this approach.

Conclusions

The rapid development of focused ion beam technologies has become an enabling factor for transmission electron microscopy applications in many different fields. Whereas the FIB preparation of TEM specimens became popular in the semiconductor field more than a decade ago, recent examples of FIB applications can be seen in a large variety of fields, from hard to soft matter and from materials to life sciences. In many application areas, there are no other TEM preparation techniques that can compete in terms of time efficiency, site specificity, and versatility. With the shorter scientific and technological cycles, TEM characterization and also related techniques can only keep pace because of the availability of this new and versatile preparation technique. However, there is also no other preparation technique with the same potential to damage the sample and to create artifacts.

In this article, we have tried to provide an overview of both the benefits and the problems of FIB preparation techniques. As experience with the specific methods and instrumental development advances, the benefits become larger whereas the detrimental factors are reduced to an extent that makes us believe that FIB milling will become the most important preparation route, even for the newest generation of sub-angstrom-resolution TEMs.

Acknowledgments

The authors thank C.A. Volkert and A.M. Minor for helpful discussions and comments. J.R. Michael was supported by Sandia National Laboratories, which is a multiprogram laboratory operated by Sandia Corporation, a Lockheed Martin Company, for the U.S. Department of Energy under contract DE-AC04–94AL85000.

References

1. L.A Giannuzzi, F.A. Stevie, *Introduction to Focused Ion Beams: Instrumentation, Theory, Techniques, and Practice* (Springer, New York, 2005).
2. E.C. Kirk et al., *Inst. Phys. Conf. Series* **100**, 501 (1989).
3. D. Basile et al., *Mater. Res. Soc. Symp. Proc.* **254** (Materials Research Society, Pittsburgh, PA, 1992) pp. 23–41.
4. M.H.F. Overwijk, F.C. van den Heuvel, C.W.T. Bull-Lieuwma, *J. Vac. Sci. Technol., B* **11**, 2021 (1993).
5. L.A. Giannuzzi et al., *Mater. Res. Soc. Symp. Proc.* **480** (Materials Research Society, Warrendale, PA, 1997) pp. 19–27.

6. T. Yaguchi, T. Kamino, T. Ishitani, R. Urao, *Microsc. Microanal*. **5**, 363 (1999).
7. L.A. Giannuzzi, R. Geurts, J. Ringnalda, *Microsc. Microanal*. **11** suppl. 2, 828 (2005).
8. L.A. Giannuzzi, F.A. Stevie, *Micron* **30**, 197 (1999).
9. F.A. Stevie et al., *Surf. Interface Anal*. **23**, 61 (1995).
10. R.M. Anderson, *Mater. Res. Soc. Symp. Proc.* **254** (Materials Research Society, Pittsburgh, PA, 1992) pp. 141–148.
11. R.M. Anderson, S.J. Klepeis, *Mater. Res. Soc. Symp. Proc*. **480** (1997) p. 187.
12. R.M. Langford, D. Ozkaya, B. Huey, A.K. Petford-Long, *Proc. Royal Microsc. Soc.: Microscopy of Semiconducting Materials XII* (2001) pp. 511–514.
13. R.J. Young, P.D. Carleson, T. Hunt, J.F. Walker, *Proc. 24th ISTFA Conf*. (1998) p. 329.
14. R.J. Young, *Microsc. Microanal. Proc*. (2000, vol. 6, suppl. 2) p. 512.
15. M.V. Moore, *Microsc. Microanal. Proc*. (2002, vol. 8, suppl. 2) p. 60.
16. R.M. Langford et al., *J. Vac. Sci. Technol. B* **19** (3), 755 (May/June 2001).
17. T. Kamino et al., *J. Electron Microsc*. **53** (6), 583 (2004).
18. T. Kamino et al., *J. Electron Microsc*. **53** (5), 563 (2004).
19. T. Ohnishi et al., *Proc. 25th Int. Symp. Testing and Failure Analysis* (November 1999) pp. 449–501.
20. L.A. Giannuzzi et al., in *Analysis Techniques of Submicron Defects, 2002 Supplement to the EDFAS Failure Analysis Desktop Reference* (ASM International, Materials Park, Ohio, 2002) pp. 29–35.
21. S.M. Schwarz, B.W. Kempshall, L.A. Giannuzzi, *Acta Mater*. **51**, 2765 (2003).
22. T. Kamino et al., *J. Electron Microsc*. **53** (5), 459 (2004).
23. J.P. McCaffrey, M.W. Phaneuf, L.D. Madsen, *Ultramicroscopy* **87**, 97 (2001).
24. Z. Wanga et al., *Appl. Surf. Sci*. **241**, 80 (2005).
25. K. Thompson et al., *Microsc. Microanal*. **12** suppl. 2, 1736CD (2006).
26. Z. Huang, *J. Microsc*. **215**, 219 (2004).
27. N.I. Kato, *J. Electron Microsc*. **53**, 451 (2004).
28. J.D. Casey et al., *J. Vac. Sci. Technol. B* **20**, 2682 (2002).
29. J.R. Michael, *Microsc. Microanal*. **12** suppl. 2, 1248CD (2006).
30. R. Spolenak, L. Sauter, C. Eberl, *Scripta Mater*. **53**, 1292 (2005).
31. S. Olliges et al., *Acta Mater*. **54**, 5393 (2006).
32. J.H. Westbrook, Ed. *Moffatt's Handbook of Binary Phase Diagrams* (Genium Group, Amsterdam, NY, 2004) p. 2/94.
33. F.A. Stevie et al., *Surf. Interface Anal*. **31**, 345 (2001).
34. W. Henschel et al., *J. Vac. Sci. Technol., B* **21**, 2975 (2003).
35. J. Mayer, T.E. Weirich, *Microsc. Microanal*. **11** suppl. 2, 46 (2005).
36. J.K. Lomness, L.A. Giannuzzi, M.D. Hampton, *Microsc. Microanal*. **7**, 418 (2001).
37. C.R. Perrey et al., *J. Microsc*. **214**, 222 (2004).
38. M. Marko et al., *J. Microsc*. **222**, 42 (2006).
39. V.G.M. Sivel et al., *J. Microsc*. **218**, 115 (2005).
40. M.K. Miller, K.F. Russell, G.B. Thompson, *Ultramicroscopy* **102**, 287 (2005).
41. D.J. Larson et al., *Ultramicroscopy* **75**, 147 (1998).
42. D.J. Larson et al., *Ultramicroscopy* **79**, 287 (1999).
43. D.J. Larson, A.K. Petford-Long, Y.Q. Ma, A. Cerezo, *Acta Mater*. **52**, 2847 (2004).
44. F. Pérez-Willard et al., *Condens. Matter*, 0601543 (2006). □